

---

# M-Walk: Learning to Walk in Graph with Monte Carlo Tree Search

---

Yelong Shen\*, Jianshu Chen<sup>†</sup>, Po-Sen Huang\*, Yuqing Gao\*, and Jianfeng Gao\*

\*Microsoft Research, Redmond, WA, USA  
 {yeshen, pshuang, yuqguo, jfgao}@microsoft.com

<sup>†</sup>Tencent AI Lab, Bellevue, WA, USA  
 jianshuchen@tencent.com

## Abstract

Learning to walk over a graph towards a target node for a given input query and a source node is an important problem in applications such as knowledge base completion (KBC). It can be formulated as a reinforcement learning (RL) problem with a known state transition model. To overcome the challenge of sparse reward, we develop a graph-walking agent called M-Walk, which consists of a deep recurrent neural network (RNN) and Monte Carlo Tree Search (MCTS). The RNN encodes the state (i.e., history of the walked path) and maps it separately to a policy, a state value and state-action Q-values. In order to effectively train the agent from sparse reward, we combine MCTS with the neural policy to generate trajectories yielding more positive rewards. From these trajectories, the network is improved in an off-policy manner using Q-learning, which modifies the RNN policy via parameter sharing. Our proposed RL algorithm repeatedly applies this policy-improvement step to learn the entire model. At test time, MCTS is again combined with the neural policy to predict the target node. Experimental results on several graph-walking benchmarks show that M-Walk is able to learn better policies than other RL-based methods, which are mainly based on policy gradients. M-Walk also outperforms traditional KBC baselines.

## 1 Introduction

We consider the problem of learning to walk over a graph in order to find a target node for a given source node and a query. Such problems appear in, for example, knowledge graph completion (KBC) [36, 16, 29, 19]. A knowledge graph is a structured representation of world knowledge in the form of entities and their relations (e.g., Figure 1(a)), and has a wide range of downstream applications such as question answering. Although a typical knowledge graph may contain millions of entities and billions of relations, it is usually far from complete. KBC aims at predicting the missing relations between entities using information from the existing knowledge graph. More formally, let  $\mathcal{G} = (\mathcal{N}, \mathcal{E})$  denote a graph, which consists of a set of nodes,  $\mathcal{N} = \{n_i\}$ , and a set of edges,  $\mathcal{E} = \{e_{ij}\}$ , that connect the nodes, and let  $q$  denote an input query. The problem is stated as using the graph  $\mathcal{G}$ , the source node  $n_S \in \mathcal{N}$  and the query  $q$  as the inputs to predict the target node  $n_T \in \mathcal{N}$ . In KBC tasks,  $\mathcal{G}$  is a given knowledge graph,  $\mathcal{N}$  is a collection of entities (nodes), and  $\mathcal{E}$  is a set of relations (edges) that connect the entities. In the example in Figure 1(a), the objective of KBC is to identify the target node  $n_T = \text{USA}$  for the given head entity  $n_S = \text{Obama}$  and the given query  $q = \text{CITIZENSHIP}$ .

The problem can also be understood as constructing a function  $f(\mathcal{G}, n_S, q)$  to predict  $n_T$ , where the functional form of  $f(\cdot)$  is generally unknown and has to be learned from a training dataset consisting

---

\*Yelong Shen, Jianshu Chen and Po-Sen Huang contributed equally to the paper.

<sup>†</sup>The work was done partially when Jianshu Chen was with Microsoft Research.



(a) An example of Knowledge Base Completion      (b) The corresponding Markov Decision Process

Figure 1: An example of Knowledge Base Completion and its formulation as a Markov Decision Process. (a) We want to identify the target node  $n_T = \text{USA}$  for a given pair of query  $q = \text{Citizenship}$  and source node  $n_S = \text{Obama}$ . (b) The activated circles and edges (in black lines) denote all the observed information up to time  $t$  (i.e., the state  $s_t$ ). The double circle denotes the current node  $n_t$ , and  $\mathcal{E}_{n_t}$  and  $\mathcal{N}_{n_t}$  denote the edges and nodes connected to the current node.

of samples like  $(n_S, q, n_T)$ . In this work, we model  $f(\mathcal{G}, n_S, q)$  by developing a graph-walking *agent* that intelligently navigates through a *subset* of nodes in the graph from  $n_S$  towards  $n_T$ . Since  $f(\cdot)$  is unknown, the problem cannot be solved by conventional search algorithms such as  $A^*$ -search [10], which seeks to find paths between the given source and target nodes. Instead, the *agent* needs to *learn* its search policy from the training dataset so that, after training is complete, the agent knows how to walk over the graph to reach the correct target node  $n_T$  for an *unseen* pair of  $(n_S, q)$ . Moreover, each training sample is in the form of “(source node, query, target node)”, and there is no intermediate supervision for the correct search path. Instead, the agent receives only delayed *evaluative* feedback: when the agent correctly (or incorrectly) predicts the target node in the training set, the agent will receive a positive (or zero) reward. For this reason, we formulate the problem as a Markov decision process (MDP) and train the agent by reinforcement learning (RL) [26].

The problem poses two major challenges. Firstly, since the state of the MDP is the entire trajectory, reaching a correct decision usually requires not just the query, but also the entire history of traversed nodes. For the KBC example in Figure 1(a), having access to the current node  $n_t = \text{Hawaii}$  alone is not sufficient to know that the best action is moving to  $n_{t+1} = \text{USA}$ . Instead, the agent must track the entire history, including the input query  $q = \text{Citizenship}$ , to reach this decision. Secondly, the reward is sparse, being received only at the end of a search path, for instance, after correctly predicting  $n_T = \text{USA}$ .

In this paper, we develop a neural graph-walking agent, named *M-Walk*, that effectively addresses these two challenges. First, M-Walk uses a novel recurrent neural network (RNN) architecture to encode the entire history of the trajectory into a vector representation, which is further used to model the policy, the state value function, and the Q-function. Second, to address the challenge of sparse reward, M-Walk exploits the fact that the MDP transition model is known and deterministic.<sup>3</sup> Specifically, it combines Monte Carlo Tree Search (MCTS) with the RNN to generate trajectories that have significantly more positive rewards than using the RNN policy alone. These trajectories can be viewed as being generated from an improved version of the RNN policy. But while these trajectories can improve the RNN policy, their off-policy nature prevents them from being leveraged by policy gradient RL methods. To solve this problem, we design a structure for sharing parameters between the Q-value network and the RNN’s policy network. This allows the policy network to be indirectly improved through Q-learning over the off-policy trajectories. Our method is in sharp contrast to existing RL-based methods for KBC, which use a policy gradients (REINFORCE) method [34] and usually require a large number of rollouts to obtain a trajectory with positive reward, especially in the early stages of learning [8, 35, 13]. Experiment results on several benchmarks, including a synthetic task and several real-world KBC tasks, show that our approach learns better policies than previous RL-based methods and traditional KBC methods.

The rest of the paper is organized as follows: Section 3 develops the M-Walk agent, including the model architecture, the training and testing (prediction) algorithms. Experiment results are presented in Section 4. Finally, we discuss related work in Section 5 and conclude the paper in Section 6.

<sup>3</sup>Whenever the agent takes an action, by selecting an edge connected to a next node, the identity of the next node (which the environment will transition to) is already known. Details can be found in Section 2.

## 2 Graph Walking as a Markov Decision Process

In this section, we formulate the graph-walking problem as a Markov Decision Process (MDP), which is defined by the tuple  $(\mathcal{S}, \mathcal{A}, \mathcal{R}, \mathcal{P})$ , where  $\mathcal{S}$  is the set of states,  $\mathcal{A}$  is the set of actions,  $\mathcal{R}$  is the reward function, and  $\mathcal{P}$  is the state transition probability. We further define  $\mathcal{S}$ ,  $\mathcal{A}$ ,  $\mathcal{R}$  and  $\mathcal{P}$  below. Figure 1(b) illustrates the MDP corresponding to the KBC of Figure 1(a). Let  $s_t \in \mathcal{S}$  denote the state at time  $t$ . Recalling that the agent needs the entire history of traversed nodes and the query to make a correct decision, we define  $s_t$  by the following recursion:

$$s_t = s_{t-1} \cup \{a_{t-1}, n_t, \mathcal{E}_{n_t}, \mathcal{N}_{n_t}\}, \quad s_0 \triangleq \{q, n_S, \mathcal{E}_{n_S}, \mathcal{N}_{n_S}\} \quad (1)$$

where  $a_t \in \mathcal{A}$  denotes the action selected by the agent at time  $t$ ,  $n_t \in \mathcal{G}$  denotes the currently visited node at time  $t$ ,  $\mathcal{E}_{n_t} \subset \mathcal{E}$  is the set of all the edges connected to  $n_t$ , and  $\mathcal{N}_{n_t} \subset \mathcal{N}$  is the set of all the nodes connected to  $n_t$  (i.e., the neighborhood). Note that state  $s_t$  is a collection of (i) all the traversed nodes (along with their edges and neighborhoods) up to time  $t$ , (ii) all the previously selected (up to time  $t - 1$ ) actions, and (iii) the initial query  $q$ . The set  $\mathcal{S}$  consists of all the possible values of  $\{s_t, t \geq 0\}$ . Based on  $s_t$ , the agent takes one of the following actions at each time  $t$ : (i) choosing an edge in  $\mathcal{E}_{n_t}$  and moving to the next node  $n_{t+1} \in \mathcal{N}_{n_t}$ , or (ii) terminating the walk (denoted as the ‘‘STOP’’ action). Once the STOP action is selected, the MDP reaches the terminal state and outputs  $\hat{n}_T = n_t$  as a prediction of the target node  $n_T$ . Therefore, we define the set of feasible actions at time  $t$  as  $\mathcal{A}_t \triangleq \mathcal{E}_{n_t} \cup \{\text{STOP}\}$ , which is usually time-varying. The entire action space  $\mathcal{A}$  is the union of all  $\mathcal{A}_t$ , i.e.,  $\mathcal{A} = \cup_t \mathcal{A}_t$ . Recall that the training set consists of samples in the form of  $(n_S, q, n_T)$ . The reward is defined to be +1 when the predicted target node  $\hat{n}_T$  is the same as  $n_T$  (i.e.,  $\hat{n}_T = n_T$ ), and zero otherwise. In the example of Figure 1(a), for a training sample (Obama, Citizenship, USA), if the agent successfully navigates from Obama to USA and correctly predicts  $\hat{n}_T = \text{USA}$ , the reward is +1. Otherwise, it will be 0. The rewards are sparse because positive reward can be received only at the end of a correct path. Furthermore, since the graph  $\mathcal{G}$  is known and static, the MDP transition probability  $p(s_t | s_{t-1}, a_{t-1})$  is *known* and *deterministic*, and is defined by (1). To see this, we observe from Figure 1(b) that once an action  $a_t$  (i.e., an edge in  $\mathcal{E}_{n_t}$  or ‘‘STOP’’) is selected, the next node  $n_{t+1}$  and its associated  $\mathcal{E}_{n_{t+1}}$  and  $\mathcal{N}_{n_{t+1}}$  are known. By (1) (with  $t$  replaced by  $t + 1$ ), this means that the next state  $s_{t+1}$  is determined. This important (model-based) knowledge will be exploited to overcome the sparse reward problem and significantly improve the performance of our method (see Sections 3–4 below).

We further define  $\pi_\theta(a_t | s_t)$ ,  $V_\theta(s_t)$  and  $Q_\theta(s_t, a_t)$  to be the policy, the state-value function, and the Q-function, respectively, where  $\theta$  is a set of model parameters. The policy  $\pi_\theta(a_t | s_t)$  denotes the probability of taking action  $a_t$  given the current state  $s_t$ . The state-value function  $V_\theta(s_t)$  characterizes the long-term reward of starting from the state  $s_t$  and following the policy  $\pi_\theta$  thereafter. And  $Q_\theta(s_t, a_t)$  defines the long-term reward of taking action  $a_t$  at state  $s_t$  and then follow the policy  $\pi_\theta$  afterwards.<sup>4</sup> The objective is to learn a policy  $\pi_\theta$  that maximizes the long-term reward  $\mathbb{E}_{s_0}[V_\theta(s_0)]$ . We now proceed to explain how to model and jointly learn  $\pi_\theta$ ,  $V_\theta$  and  $Q_\theta$  to achieve this objective.

## 3 The M-Walk Agent

In this section, we develop a neural graph-walking agent named M-Walk (i.e., MCTS for graph Walking), which consists of (i) a novel neural architecture for jointly modeling  $\pi_\theta$ ,  $V_\theta$  and  $Q_\theta$ , and (ii) Monte Carlo Tree Search (MCTS). We first introduce the overall neural architecture, and then explain how MCTS is used during the training and testing stages. Finally, we describe some further details of the neural architecture. Our discussion focuses on addressing the two challenges described earlier: history-dependent state and sparse rewards.

### 3.1 The neural architecture for jointly modeling $\pi_\theta$ , $V_\theta$ and $Q_\theta$

Recall from previous sections (e.g., eqn. (1)) that one challenge in applying RL to the graph-walking problem is that the state  $s_t$  nominally includes the entire history of observations. To address this problem, we propose a special RNN encoding the state  $s_t$  at each time  $t$  into a vector representation,  $h_t = \text{ENC}_{\theta_e}(s_t)$ , where  $\theta_e$  is the associated model parameter. We defer the discussion of this RNN state encoder to Section 3.4, and focus in this section on how to use  $h_t$  to jointly model  $\pi_\theta$ ,  $V_\theta$

<sup>4</sup>A more precise notation would be  $V_\theta^\pi(s_t)$  and  $Q_\theta^\pi(s_t, a_t)$ . For simplicity, we drop the superscript  $\pi$ .



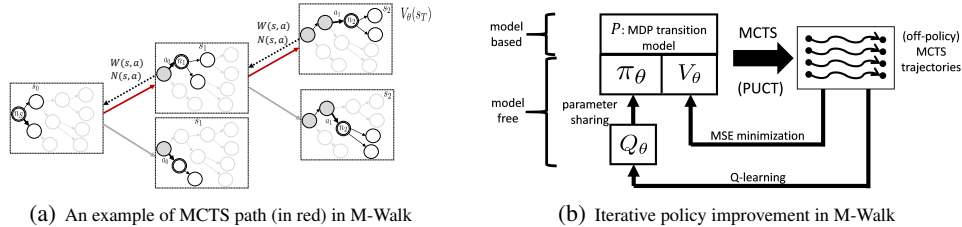


Figure 3: MCTS is used to generate trajectories for iterative policy improvement in M-Walk.

$(s, a)$ -th edge on the MCTS tree. Overall, PUCT treats  $\pi_\theta$  as a prior probability to bias the MCTS search; PUCT initially prefers actions with high values of  $\pi_\theta$  and low visit count  $N(s, a)$ , but then asymptotically prefers actions with high value (i.e.,  $W(s, a)/N(s, a)$ ). When PUCT selects the STOP action or the maximum search horizon has been reached, MCTS completes one simulation and updates  $W(s, a)$  and  $N(s, a)$  using  $V_\theta$ . (See Figure 3(a) for an example and Appendix B.1 for more details.) The key idea of our method is that running multiple MCTS simulations generates a set of trajectories with more positive rewards (see Section 4 for more analysis), which can also be viewed as being generated by an improved policy of  $\pi_\theta$ . Therefore, learning from these trajectories can further improve  $\pi_\theta$ . Our RL algorithm repeatedly applies this policy-improvement step to refine the policy. However, since these trajectories are generated by a policy that is different from  $\pi_\theta$ , they are off-policy data, breaking the assumptions inherent in policy gradient methods. For this reason, we instead update the Q-network from these trajectories in an off-policy manner using Q-learning:  $\theta \leftarrow \theta + \alpha \cdot \nabla_\theta Q_\theta(s_t, a_t) \times (r(s_t, a_t) + \gamma \max_{a'} Q_\theta(s_{t+1}, a') - Q_\theta(s_t, a_t))$ . Recall from Section 3.1 that  $\pi_\theta$  and  $Q_\theta(s, a)$  share the same set of model parameters; once the Q-network is updated, the policy network  $\pi_\theta$  will also be automatically improved. Meanwhile, the value network  $V_\theta(s)$  is updated by minimizing the mean-square-error  $\mathbb{E}|r(s_T, a_T) - V_\theta(s_T)|^2$ . Note that the value network is only trained and used to evaluate the terminal MCTS states. Finally, the new  $\pi_\theta$  is used to control the MCTS in the next iteration. The main idea of the training algorithm is summarized in Figure 3(b).

### 3.3 The prediction algorithm

At test time, we want to infer the target node  $n_T$  for an unseen pair of  $(n_S, q)$ . One approach is to use the learned policy  $\pi_\theta$  to walk through the graph  $\mathcal{G}$  to find  $n_T$ . However, this would not exploit the known MDP transition model (1). Instead, we combine the learned  $\pi_\theta$  and  $V_\theta$  with MCTS to generate an MCTS search tree, as in the training stage. Note that there could be multiple paths that reach the same terminal node  $n \in \mathcal{G}$ , meaning that there could be multiple leaf states in MCTS corresponding to that node. Therefore, the prediction results from these MCTS leaf states need to be merged into one score to rank the node  $n$ . Specifically, we use  $\text{Score}(n) = \sum_{s_T \rightarrow n} N(s_T, a_T) / N \times V_\theta(s_T)$ , where  $N$  is the total number of MCTS simulations, and the summation is over all the leaf states  $s_T$  that correspond to the same node  $n \in \mathcal{G}$ .  $\text{Score}(n)$  is a weighted average of the terminal state values associated with the same candidate node  $n$ .<sup>6</sup> Among all the candidates nodes, we pick the predicted target node to be the one with the highest score:  $\hat{n}_T = \text{argmax}_n \text{Score}(n)$ .

### 3.4 The RNN state encoder

We now discuss the details of the RNN state encoder  $h_t = \text{ENC}_{\theta_e}(s_t)$ . Specifically, we explain how the sub-vectors of  $h_t$  are computed. We introduce  $q_t \triangleq s_{t-1} \cup \{a_{t-1}, n_t\}$  as an auxiliary variable. Then, the state  $s_t$  in (1) can be written as  $s_t = q_t \cup \{\mathcal{E}_{n_t}, \mathcal{N}_{n_t}\}$ . Note that the state  $s_t$  is composed of two parts: (i)  $\mathcal{E}_{n_t}$  and  $\mathcal{N}_{n_t}$ , which represent the candidate actions to be selected (excluding the STOP action), and (ii)  $q_t$ , which represents the history. We use two different neural networks to encode these separately. For the  $n'$ -th candidate action ( $n' \in \mathcal{N}_{n_t}$ ), we concatenate  $n'$  with its associated  $e_{n_t, n'} \in \mathcal{E}_{n_t}$  and input them into a fully connected network (FCN)  $f_{\theta_A}(\cdot)$  to compute their joint vector representation  $h_{n', t}$ , where  $\theta_A$  is the model parameter. Recall that the action space  $\mathcal{A}_t = \mathcal{E}_{n_t} \cup \{\text{STOP}\}$  can be time-varying when the size of  $\mathcal{E}_{n_t}$  changes over time. To address this

<sup>6</sup>There could be alternative ways to compute the score, such as  $\text{Score}(n) = \max_{s_T \rightarrow n} V_\theta(s_T)$ . However, we found in our (unreported) experiments that they do not make much difference.

issue, we apply the same FCN  $f_\theta(\cdot)$  to different  $(n', e_{n_t, n'})$  to obtain their respective representations. Then, we use a coordinate-wise max-pooling operation over  $\{h_{n', t} : n' \in \mathcal{N}_{n_t}\}$  to obtain a (fixed-length) overall vector representation of  $\{\mathcal{E}_{n_t}, \mathcal{N}_{n_t}\}$ . To encode  $q_t$ , we call upon the following recursion for  $q_t$  (see Appendix A for the derivation):  $q_{t+1} = q_t \cup \{\mathcal{E}_{n_t}, \mathcal{N}_{n_t}, a_t, n_{t+1}\}$ . Inspired by this recursion, we propose using the GRU-RNN [4] to encode  $q_t$  into a vector representation<sup>7</sup>:  $q_{t+1} = f_{\theta_q}(q_t, [h_{A,t}, h_{a_t,t}, n_{t+1}])$  with initialization  $q_0 = f_{\theta_q}(q, [0, 0, n_S])$ , where  $\theta_q$  is the model parameter, and  $h_{a_t,t}$  denotes the vector  $h_{n', t}$  at  $n' = a_t$ . We use  $h_{A,t}$  and  $h_{a_t,t}$  computed by the FCNs to represent  $(\mathcal{E}_{n_t}, \mathcal{N}_{n_t})$  and  $a_t$ , respectively. Then, we map  $q_t$  to  $h_{S,t}$  using another FCN  $f_{\theta_S}(\cdot)$ . Figure 2(b) illustrates the overall architecture of the RNN state encoder, with  $\theta_e \triangleq \{\theta_A, \theta_S, \theta_q\}$ .

## 4 Experiments

We evaluate and analyze the effectiveness of M-Walk on a synthetic Three Glass Puzzle task, and two real-world KBC tasks. We briefly describe the tasks here, and give the experiment details and hyperparameters in Appendix B.

**Three Glass Puzzle** The Three Glass Puzzle [20] is a problem studied in math puzzles and graph theory. It involves three milk containers  $A$ ,  $B$  and  $C$ , with capacities  $A$ ,  $B$ , and  $C$  liters, respectively. The containers display no intermediate markings. There are three feasible actions at each time step: (i) *fill* a container (to its capacity), (ii) *empty* all of its liquid, and (iii) *pour* its liquid into another container (up to its capacity). The objective of the problem is, given a desired volume  $q$ , to take a sequence of actions on the three containers after which one of them contains  $q$  liters of liquid. We formulate this as a graph-walking problem; in the graph  $\mathcal{G}$ , each node  $n = (a, b, c)$  denotes the amounts of remaining liquid in the three containers, each edge denotes one of the three feasible actions, and the input query is the desired volume  $q$ . The reward is  $+1$  when the agent successfully fills one of the containers to  $q$  and zero otherwise. See Appendix B.2.1 for the dataset details. We use the vanilla policy gradient (REINFORCE) [34] as the baseline, and the task success rate as the evaluation metric.

**Knowledge Base Completion** We use WN18RR and NELL995 knowledge graph datasets for evaluation. The WN18RR [6] is created from the original WN18 [2] by removing various sources of test leakage, making the datasets more challenging. The NELL-995 dataset is released by [36] and has separate graphs for each query relation. We use the same data split and preprocessing protocol as in [6] for WN18RR, and in [36, 5] for NELL995. As in [36, 5], we study the 10 relation tasks of NELL995 separately. We use Hits@1,3 and mean reciprocal rank (MRR) as the evaluation metrics for WN18RR, and use mean average precision (MAP) for NELL995 (to be consistent with [36, 5]), where Hits@ $K$  computes the percentage of the desired entities being ranked among the top- $K$  list and MRR computes an average of the reciprocal rank of the desired entities. We compare against RL-based methods [36, 5], embedding-based models (including DistMult [37], ComplEx [30] and ConvE [6]) and the recent work in logical rules (NeuralLP) [38]. For all the baseline methods, we used the implementation released by the corresponding authors with their best reported hyperparameter settings.<sup>8</sup> The details of the hyperparameters for M-Walk are described in Appendix B.2.2.

### 4.1 Performance of M-Walk

We first report the overall performance of the M-Walk algorithm on the three tasks, and compare it with other baseline methods. We run the experiments three times and report the means and standard deviations (except for PRA, TransE and TransR on NELL995, whose results are directly quoted from [36]). On the Three Glass Puzzle task, M-Walk significantly outperforms the baseline: the best model of M-Walk achieves an accuracy of  $(99.0 \pm 1.0)\%$  while the best REINFORCE method achieves  $(49.0 \pm 2.6)\%$  (see Appendix C for more experiments with different settings on this task). For the two KBC tasks, we report their results in Tables 1-2, where PG-Walk and Q-Walk are two methods we created *just for ablation study* in the next section. The proposed method outperforms previous works in most of the metrics across both KBC datasets.

<sup>7</sup>For simplicity, we use the same notation  $q_t$  to denote its vector representation.

<sup>8</sup>ConvE: <https://github.com/TimDettmers/ConvE>, Neural-LP: <https://github.com/fanyangxyz/Neural-LP/>, DeepPath: <https://github.com/xwhan/DeepPath>, MINERVA: <https://github.com/shehzaazd/MINERVA/>

Table 1: The MAP scores (%) on NELL995 task, where we report RL based methods in terms of “mean (standard deviation)”. PG-Walk and Q-Walk are methods we created just for ablation study.

Tasks	M-Walk	PG-Walk	Q-Walk	MINERVA	DeepPath	PRA	TransE	TransR
athletePlaysForTeam	<b>84.7</b> (1.3)	80.8 (0.9)	82.6 (1.2)	82.7 (0.8)	72.1 (1.2)	54.7	62.7	67.3
athletePlaysInLeague	<b>97.8</b> (0.2)	96.0 (0.6)	96.2 (0.8)	95.2 (0.8)	92.7 (5.3)	84.1	77.3	91.2
athleteHomeStadium	91.9 (0.1)	91.9 (0.3)	91.1 (1.3)	<b>92.8</b> (0.1)	84.6 (0.8)	85.9	71.8	72.2
athletePlaysSport	98.3 (0.1)	98.0 (0.8)	97.0 (0.2)	<b>98.6</b> (0.1)	91.7 (4.1)	47.4	87.6	96.3
teamPlaySports	<b>88.4</b> (1.8)	87.4 (0.9)	78.5 (0.6)	87.5 (0.5)	69.6 (6.7)	79.1	76.1	81.4
orgHeadquarterCity	<b>95.0</b> (0.7)	94.0 (0.4)	94.0 (0.6)	94.5 (0.3)	79.0 (0.0)	81.1	62.0	65.7
worksFor	<b>84.2</b> (0.6)	84.0 (1.6)	82.7 (0.2)	82.7 (0.5)	69.9 (0.3)	68.1	67.7	69.2
bornLocation	81.2 (0.0)	<b>82.3</b> (0.6)	81.4 (0.5)	78.2 (0.0)	75.5 (0.5)	66.8	71.2	81.2
personLeadsOrg	<b>88.8</b> (0.5)	87.2 (0.5)	86.9 (0.5)	83.0 (2.6)	79.0 (1.0)	70.0	75.1	77.2
orgHiredPerson	<b>88.8</b> (0.6)	87.2 (0.4)	87.8 (0.9)	87.0 (0.3)	73.8 (1.9)	59.9	71.9	73.7
Overall	<b>89.9</b>	88.9	87.8	87.6	78.8	69.7	72.3	77.5

Table 2: The results on the WN18RR dataset, in the form of “mean (standard deviation)”.

Metric (%)	M-Walk	PG-Walk	Q-Walk	MINERVA	ComplEx	ConvE	DistMult	NeuralLP
HITS@1	<b>41.4</b> (0.1)	39.3 (0.2)	38.2 (0.3)	35.1 (0.1)	38.5 (0.3)	39.6 (0.3)	38.4 (0.4)	37.2 (0.1)
HITS@3	44.5 (0.2)	41.9 (0.1)	40.8 (0.4)	44.5 (0.4)	43.9 (0.3)	<b>44.7</b> (0.2)	42.4 (0.3)	43.4 (0.1)
MRR	<b>43.7</b> (0.1)	41.3 (0.1)	40.1 (0.3)	40.9 (0.1)	42.2 (0.2)	43.3 (0.2)	41.3 (0.3)	43.5 (0.1)

## 4.2 Analysis of M-Walk

We now perform extensive experimental analysis to understand the proposed M-Walk algorithm, including (i) the contributions of different components, (ii) its ability to overcome sparse rewards, (iii) hyperparameter analysis, and (iv) its strengths and weaknesses compared to traditional KBC methods. First, we use ablation studies to analyze the contributions of different components in M-Walk. To understand the contribution of the proposed neural architecture in M-Walk, we create a method, PG-Walk, which uses the same neural architecture as M-Walk but with the same training (PG) and testing (beam search) algorithms as MINERVA [5]. We observe that the novel neural architecture of M-Walk contributes an overall 1% gain relative to MINERVA on NELL995, and it is still 1% worse than M-Walk, which uses MCTS at training and testing. To further understand the contribution of MCTS, we create another method, Q-Walk, which uses the same model architecture as M-Walk except that it is trained by Q-learning only without MCTS. Note that this lost about 2% in overall performance on NELL995. We observe similar trends on WN18RR. In addition, we also analyze the importance of MCTS in the testing stage in Appendix C.1. Second, we analyze the ability of M-Walk to overcome the sparse rewards problem. In Figures 4-5, we show the positive reward rate (i.e., percentage of trajectories with positive reward during training) on the Three Glass Puzzle task and the NELL995 tasks. Compared to the policy gradient method (PG-Walk), and Q-learning method (Q-Walk) methods under the same model architecture, M-Walk with MCTS is able to generate trajectories with more positive rewards, and this continues to improve as training progresses. This confirms our motivation of using MCTS to generate higher-quality trajectories to alleviate the sparse reward problem in graph walking. Third, we analyze the performance of M-Walk under different numbers of MCTS rollout simulations and different search horizons on WN18NN dataset, with the results shown in Figure 6(a). We observe that the model is less sensitive to search horizon and is more sensitive to the number of MCTS rollouts. Finally, we analyze the strengths and weaknesses of M-Walk relative to traditional methods on the WN18NN dataset. The first question is how M-Walk performs on reasoning paths of different lengths compared to baselines. To answer this, we analyze the Hits@1 accuracy against ConvE in Fig. 6(b). We categorize each test example using the BFS (breadth-first search) steps from the query entity to the target entity (-1 means not reachable). We observe that M-Walk outperforms the strong baseline ConvE by 4.6–10.9% in samples that require 2 and 3 steps, while almost on par for paths of length one. Therefore, M-Walk is better at reasoning over longer paths than ConvE. Another question is what are the major types of errors made by M-Walk. Recall that M-Walk only walks through a subset of the graph and ranks a subset of candidate nodes (e.g., MCTS produces about 20–60 unique candidates on WN18RR). When the ground truth is not in the candidate set, M-Walk always makes mistakes. To examine its effect, we show in Figure 6(c)-top the HITS@K accuracies when the ground truth is in the candidate

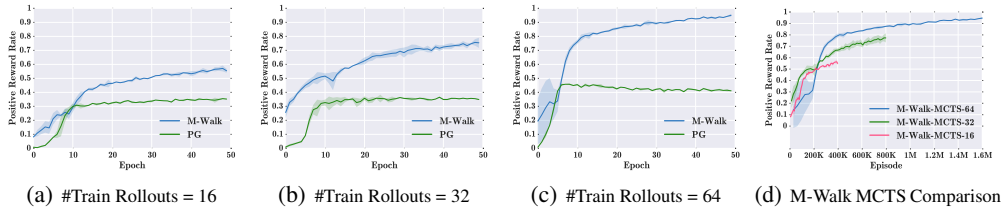


Figure 4: The positive reward rate during training on Three Glass Puzzle task.

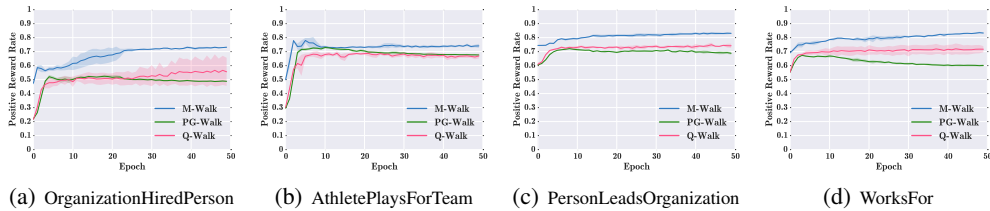


Figure 5: The positive reward rate on the NELL-995 task. (See Appendix C.1.1 for more results.)

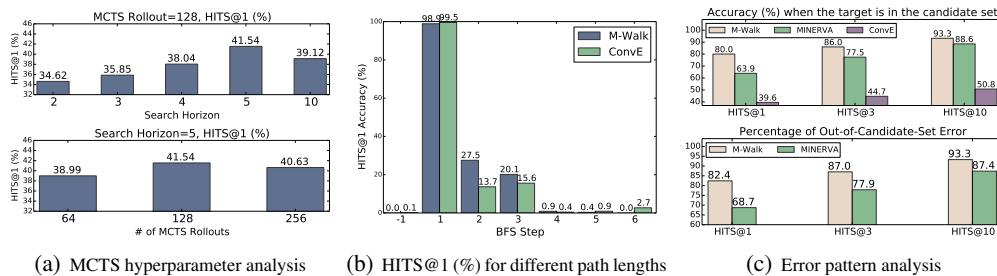


Figure 6: M-Walk hyperparameter and error analysis on WN18RR.

set.<sup>9</sup> It shows that M-Walk has very high accuracy in this case, which is significantly higher than ConvE (80% vs 39.6% in HITS@1). We further examine the percentage of out-of-candidate-set error among all errors in Figure 6(c)-bottom. It shows that the major error made by M-Walk is the out-of-candidate-set error. These observations point to an important direction for improving M-Walk in future work: increasing the chance of covering the target by the candidate set.

## 5 Related Work

**Reinforcement Learning** Recently, deep reinforcement learning has achieved great success in many artificial intelligence problems [17, 23, 24]. The use of deep neural networks with RL allows policies to be learned from raw data (e.g., images) in an end-to-end manner. Our work also aligns with this direction. Furthermore, the idea of using an RNN to encode the history of observations also appeared in [11, 33]. The combination of model-based and model-free information in our work shares the same spirit as [23, 24, 25, 32]. Among them, the most relevant ones are [23, 24], which combine MCTS with neural policy and value functions to achieve superhuman performance on Go. Different from our work, the policy and the value networks in [23] are trained separately without the help of MCTS, and are only used to help MCTS after being trained. The work [24] uses a new policy iteration method that combines the neural policy and value functions with MCTS during training. However, the method in [24] improves the policy network from the MCTS probabilities of the moves, while our method improves the policy from the trajectories generated by MCTS. Note that the former is constructed from the visit counts of all the edges connected to the MCTS root node; it only uses

<sup>9</sup>The ground truth is always in the candidate list in ConvE, as it examines all the nodes.

information near the root node to improve the policy. By contrast, we improve the policy by learning from the trajectories generated by MCTS, using information over the entire MCTS search tree.

**Knowledge Base Completion** In KBC tasks, early work [2] focused on learning vector representations of entities and relations. Recent approaches have demonstrated limitations of these prior approaches: they suffer from cascading error when dealing with compositional (multi-step) relationships [9]. Hence, recent work [7, 18, 9, 15, 28] proposed approaches for injecting multi-step paths such as random walks through sequences of triples during training, further improving performance in KBC tasks. IRN [22] and Neural LP [38] explore multi-step relations by using an RNN controller with attention over an external memory. Compared to RL-based approaches, it is hard to interpret the traversal paths, and these models can be computationally expensive to access the entire graph in the memory [22]. Two recent works, DeepPath [36] and MINERVA [5], use RL-based approaches to explore paths in knowledge graphs. DeepPath requires target entity information in the state representation and uses the gathered paths from RL to the Path Ranking Algorithm [14]. MINERVA [5] uses a policy gradient method to explore paths during training and test. Our proposed model further exploits state transition information by integrating the MCTS algorithm. Empirically, our proposed algorithm outperforms both DeepPath and MINERVA in the KBC benchmarks.

## 6 Conclusion and Discussion

We developed an RL-agent (M-Walk) that learns to walk over a graph towards a desired target node for a given pair of input query and source node. Specifically, we proposed a novel neural architecture that encodes the state into a vector representation and maps it into a Q-network (for the policy), and a value network. To learn from sparse rewards, we propose a new reinforcement learning algorithm, which alternates between an MCTS trajectory generation step and a policy improvement step, to iteratively refine the policy. At test time, the learned networks are combined with MCTS to search for the target node. Experiment results on several benchmarks demonstrate that our method learns better policies compared to other baseline methods, including RL-based and traditional methods on KBC tasks. Furthermore, we also performed extensive experimental analysis to understand M-Walk. We found that our method is more accurate when the groundtruth is in the candidate set. We also found that the out-of-candidate-set error is the main type of error made by M-Walk. Therefore, in future work, we intend to improve this method by reducing such out-of-candidate-set errors.

## References

- [1] Irwan Bello, Hieu Pham, Quoc V Le, Mohammad Norouzi, and Samy Bengio. Neural combinatorial optimization with reinforcement learning. *arXiv preprint arXiv:1611.09940*, 2016.
- [2] Antoine Bordes, Nicolas Usunier, Alberto Garcia-Duran, Jason Weston, and Oksana Yakhnenko. Translating embeddings for modeling multi-relational data. In *Proc. NIPS*, pages 2787–2795, 2013.
- [3] Jianshu Chen, Chong Wang, Lin Xiao, Ji He, Lihong Li, and Li Deng. Q-LDA: Uncovering latent patterns in text-based sequential decision processes. In *Proc. NIPS*, pages 4984–4993, 2017.
- [4] Kyunghyun Cho, Bart Van Merriënboer, Caglar Gulcehre, Dzmitry Bahdanau, Fethi Bougares, Holger Schwenk, and Yoshua Bengio. Learning phrase representations using rnn encoder-decoder for statistical machine translation. *Proc. EMNLP*, 2014.
- [5] Rajarshi Das, Shehzaad Dhuliawala, Manzil Zaheer, Luke Vilnis, Ishan Durugkar, Akshay Krishnamurthy, Alexander J. Smola, and Andrew McCallum. Go for a walk and arrive at the answer: Reasoning over paths in knowledge bases using reinforcement learning. In *Proc. ICLR*, 2018.
- [6] Tim Dettmers, Minervini Pasquale, Stenertorp Pontus, and Sebastian Riedel. Convolutional 2D knowledge graph embeddings. In *Proc. AAAI*, February 2018.
- [7] Matt Gardner, Partha Pratim Talukdar, Jayant Krishnamurthy, and Tom Mitchell. Incorporating vector space similarity in random walk inference over knowledge bases. In *EMNLP*, 2014.
- [8] Shixiang Gu, Timothy Lillicrap, Zoubin Ghahramani, Richard E Turner, and Sergey Levine. Q-prop: Sample-efficient policy gradient with an off-policy critic. In *Proc. ICLR*, 2016.

- [9] Kelvin Guu, John Miller, and Percy Liang. Traversing knowledge graphs in vector space. In *Proc. EMNLP*, 2015.
- [10] Peter E Hart, Nils J Nilsson, and Bertram Raphael. A formal basis for the heuristic determination of minimum cost paths. *IEEE Trans. Systems Science and Cybernetics*, 4(2):100–107, 1968.
- [11] Matthew J. Hausknecht and Peter Stone. Deep recurrent Q-learning for partially observable MDPs. *CoRR*, abs/1507.06527, 2015.
- [12] Ji He, Jianshu Chen, Xiaodong He, Jianfeng Gao, Lihong Li, Li Deng, and Mari Ostendorf. Deep reinforcement learning with a natural language action space. In *Proc. ACL*, pages 1621–1630, 2016.
- [13] Sham M Kakade. A natural policy gradient. In *Proc. NIPS*, pages 1531–1538, 2002.
- [14] Ni Lao, Tom Mitchell, and William W Cohen. Random walk inference and learning in a large scale knowledge base. In *Proc. EMNLP*, pages 529–539, 2011.
- [15] Yankai Lin, Zhiyuan Liu, Huanbo Luan, Maosong Sun, Siwei Rao, and Song Liu. Modeling relation paths for representation learning of knowledge bases. In *EMNLP*, 2015.
- [16] Yankai Lin, Zhiyuan Liu, Maosong Sun, Yang Liu, and Xuan Zhu. Learning entity and relation embeddings for knowledge graph completion. In *AAAI*, 2015.
- [17] Volodymyr Mnih, Koray Kavukcuoglu, David Silver, Andrei A Rusu, Joel Veness, Marc G Bellemare, Alex Graves, Martin Riedmiller, Andreas K Fidjeland, Georg Ostrovski, et al. Human-level control through deep reinforcement learning. *Nature*, 518(7540):529, 2015.
- [18] Arvind Neelakantan, Benjamin Roth, and Andrew McCallum. Compositional vector space models for knowledge base completion. In *Proc. AAAI*, 2015.
- [19] Maximilian Nickel, Volker Tresp, and Hans-Peter Kriegel. A three-way model for collective learning on multi-relational data. In *Proc. ICML*, pages 809–816, 2011.
- [20] Oystein Ore. *Graphs and Their Uses*, volume 34. Cambridge University Press, 1990.
- [21] Christopher D. Rosin. Multi-armed bandits with episode context. *Annals of Mathematics and Artificial Intelligence*, 61(3):203–230, Mar 2011.
- [22] Yelong Shen, Po-Sen Huang, Ming-Wei Chang, and Jianfeng Gao. Modeling large-scale structured relationships with shared memory for knowledge base completion. In *Proceedings of the 2nd Workshop on Representation Learning for NLP*, pages 57–68, 2017.
- [23] David Silver, Aja Huang, Chris J Maddison, Arthur Guez, Laurent Sifre, George Van Den Driessche, Julian Schrittwieser, Ioannis Antonoglou, Veda Panneershelvam, Marc Lanctot, et al. Mastering the game of Go with deep neural networks and tree search. *Nature*, 529(7587):484–489, 2016.
- [24] David Silver, Julian Schrittwieser, Karen Simonyan, Ioannis Antonoglou, Aja Huang, Arthur Guez, Thomas Hubert, Lucas Baker, Matthew Lai, Adrian Bolton, et al. Mastering the game of Go without human knowledge. *Nature*, 550(7676):354, 2017.
- [25] David Silver, Hado van Hasselt, Matteo Hessel, Tom Schaul, Arthur Guez, Tim Harley, Gabriel Dulac-Arnold, David Reichert, Neil Rabinowitz, Andre Barreto, and Thomas Degris. The predictron: End-to-end learning and planning. In *Proc. ICML*, 2017.
- [26] Richard S Sutton and Andrew G Barto. *Reinforcement Learning: An Introduction*, volume 1. MIT press Cambridge, 1998.
- [27] Richard S Sutton, David A McAllester, Satinder P Singh, and Yishay Mansour. Policy gradient methods for reinforcement learning with function approximation. In *Proc. NIPS*, pages 1057–1063, 2000.
- [28] Kristina Toutanova, Xi Victoria Lin, Scott Wen tau Yih, Hoifung Poon, and Chris Quirk. Compositional learning of embeddings for relation paths in knowledge bases and text. In *Proc. ACL*, 2016.
- [29] Théo Trouillon, Christopher R Dance, Johannes Welbl, Sebastian Riedel, Éric Gaussier, and Guillaume Bouchard. Knowledge graph completion via complex tensor factorization. *Journal of Machine Learning Research*, 2017.
- [30] Théo Trouillon, Johannes Welbl, Sebastian Riedel, Éric Gaussier, and Guillaume Bouchard. Complex embeddings for simple link prediction. In *Proc. ICML*, pages 2071–2080, 2016.

- [31] Oriol Vinyals, Meire Fortunato, and Navdeep Jaitly. Pointer networks. In *Proc. NIPS*, pages 2692–2700, 2015.
- [32] Theophane Weber, Sébastien Racanière, David P. Reichert, Lars Buesing, Arthur Guez, Danilo Jimenez Rezende, Adrià Puigdomènech Badia, Oriol Vinyals, Nicolas Heess, Yujia Li, Razvan Pascanu, Peter Battaglia, David Silver, and Daan Wierstra. Imagination-augmented agents for deep reinforcement learning. In *Proc. NIPS*, 2017.
- [33] Daan Wierstra, Alexander Förster, Jan Peters, and Jürgen Schmidhuber. Recurrent policy gradients. *Logic Journal of the IGPL*, 18(5):620–634, 2010.
- [34] Ronald J Williams. Simple statistical gradient-following algorithms for connectionist reinforcement learning. In *Reinforcement Learning*, pages 5–32. Springer, 1992.
- [35] Yuhuai Wu, Elman Mansimov, Roger B Grosse, Shun Liao, and Jimmy Ba. Scalable trust-region method for deep reinforcement learning using kronecker-factored approximation. In *Proc. NIPS*, pages 5285–5294, 2017.
- [36] Wenhao Xiong, Thien Hoang, and William Yang Wang. DeepPath: A reinforcement learning method for knowledge graph reasoning. In *Proc. EMNLP*, pages 575–584, 2017.
- [37] Bishan Yang, Wen-tau Yih, Xiaodong He, Jianfeng Gao, and Li Deng. Embedding entities and relations for learning and inference in knowledge bases. In *ICLR*, 2015.
- [38] Fan Yang, Zhilin Yang, and William W Cohen. Differentiable learning of logical rules for knowledge base reasoning. In *Proc. NIPS*, pages 2316–2325, 2017.

## A Derivation of the recursion for $q_t$

Recalling the definition  $q_t \triangleq s_{t-1} \cup \{a_{t-1}, n_t\}$  and using the recursion (1), we have

$$\begin{aligned} q_{t+1} &\stackrel{(a)}{=} s_t \cup \{a_t, n_{t+1}\} \\ &\stackrel{(b)}{=} s_{t-1} \cup \{a_{t-1}, n_t, \mathcal{E}_{n_t}, \mathcal{N}_{n_t}\} \cup \{a_t, n_{t+1}\} \\ &\stackrel{(c)}{=} q_t \cup \{\mathcal{E}_{n_t}, \mathcal{N}_{n_t}, a_t, n_{t+1}\} \end{aligned}$$

where step (a) uses the definition of  $q_{t+1}$ , step (b) substitutes the recursion (1), and step (c) uses the definition of  $q_t$ .

## B Algorithm Implementation Details

The detailed algorithm of ReinforceWalk is described in Algorithm 1.

---

### Algorithm 1 ReinforceWalk Training Algorithm

---

- 1: **Input:** Graph  $\mathcal{G}$ ; Initial node  $n_S$ ; Query  $q$ ; Target node  $n_T$ ; Maximum Path Length  $T_{\max}$ ; MCTS Search Number  $E$ ;
- 2: **for** episode  $e$  in  $[1..E]$  **do**
- 3:   Set current node  $n_0 = n_S$ ;  $q_0 = f_{\theta_q}(q, 0, 0, n_0)$
- 4:   **for**  $t = 0 \dots T_{\max}$  **do**
- 5:     Lookup from dictionary to obtain  $W(s_t, a)$  and  $N(s_t, a)$
- 6:     Select the action  $a_t$  with the maximum PUCT value:
 
$$a_t = \operatorname{argmax}_a \left\{ c \cdot \pi_{\theta}(a|s_t)^{\beta} \frac{\sqrt{\sum_{a'} N(s_t, a')}}{1 + N(s_t, a)} + \frac{W(s_t, a)}{N(s_t, a)} \right\}$$
- 7:     Update  $q_{t+1} = f_{\theta_q}(q_t, h_{A,t}, h_{a_t,t}, n_{t+1})$
- 8:     **if**  $a_t$  is STOP **then**
- 9:       Compute estimated reward value  $V_{\theta}(s_t)$
- 10:      Add generated path  $p$  into a path list
- 11:      Backup along the path  $p$  to update visit count  $W(s_t, a)$  and  $N(s_t, a)$
- 12:      **Break**
- 13:     **end if**
- 14:   **end for**
- 15: **end for**
- 16: **for** each path  $p$  in the path list **do**
- 17:   Set reward  $r = 1$  if the end of the path  $n_t = n_T$  otherwise  $r = 0$
- 18:   Repeatedly update the model parameters with Q-learning:

$$\theta \leftarrow \theta + \alpha \cdot \nabla_{\theta} Q_{\theta}(s_t, a_t) \times \left( r(s_t, a_t) + \gamma \max_{a'} Q_{\theta}(s_{t+1}, a') - Q_{\theta}(s_t, a_t) \right)$$

Repeatedly update the Reward Estimation Network by minimizing the MSE loss:

$$\min_{\theta} \mathbb{E}(r(s_T, a_T) - V_{\theta}(s_T))^2$$

- 19: **end for**
- 

### B.1 MCTS implementation

In the MCTS implementation, we maintain a lookup table to record values  $W(s_t, a)$  and  $N(s_t, a)$  for each visited state-action pair. The state  $s_t$  in the graph walk problem contains all the information along the traversal path, and  $n_t$  is the node at the current step  $t$ . We assign an index  $i_a$  to each candidate action  $a$  from  $n_t$ , indicating  $a$  is the  $i_a$ -th action of the node  $n_t$ . Thus the state  $s_t$  can be encoded as a path string  $P_{s_t} = (q, n_0, i_{a_0}, n_1, i_{a_1}, \dots, n_t)$ . We build a dictionary  $\mathcal{D}$  using the path

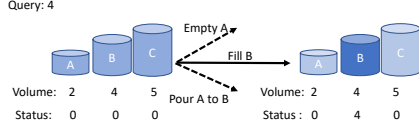


Figure 7: Graph traversal in Three Glass Puzzle problem

string as a key and we record  $W(s_t, a)$  and  $N(s_t, a)$  as values in  $\mathcal{D}$ . In the backup stage, the  $W(s_t, a)$  and  $N(s_t, a)$  values are updated for each state-action pair along with the traversal path in MCTS:

$$N(s_t, a) = N(s_t, a) + \gamma^{L-t}$$

$$W(s_t, a) = W(s_t, a) + \gamma^{L-t} V_\theta(s_L),$$

where  $L$  is the length of the traversal path, and  $\gamma$  is the discount factor of the MDP.

## B.2 Experiment details

### B.2.1 Three Glass Puzzle

**An example** Figure 7 gives a concrete example of the Three Glass Puzzle, where an action sequence is shown to reach the desired volume of 4. We denote  $a, b, c$  as the current volumes of the containers. To achieve the target  $q = 1$ , we can take the following action sequences: For example,  $(A = 8, B = 5, C = 3), q = 4$ . All three containers start empty. The following action sequences are one solution:

- Initial state  $\rightarrow (a = 0, b = 0, c = 0)$
- Fill the second container  $\rightarrow (a = 0, b = 5, c = 0)$
- From the second to first  $\rightarrow (a = 4, b = 1, c = 0)$
- Empty the third container  $\rightarrow (a = 0, b = 2, c = 0)$
- From second to third  $\rightarrow (a = 0, b = 0, c = 2)$
- Fill the second container  $\rightarrow (a = 0, b = 5, c = 2)$
- From second to third  $\rightarrow (a = 0, b = 4, c = 3)$

**Data generation** In the Three Glass Puzzle experiments, we randomly draw four integers from  $[1, 50)$  to represent the capacities  $A, B, C$ , and the desired volume  $q$ . We further restrict the values so that  $A \leq B \leq C$  and  $q < C$ , to avoid data duplication. We discard puzzles for which there is no solution. Finally, we keep 600 unique puzzles as the experimental dataset, where 500 puzzles are used for training and the other 100 are used to test a model’s generalization capability on the unseen test set.

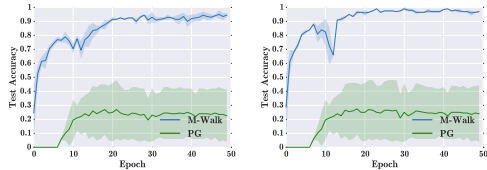
**Experiment settings and hyperparameters** Let  $a, b, c$  be the current status of each container, and define the puzzle status at step  $t$  as  $n_t = [I_A^T, I_B^T, I_C^T, I_a^T, I_b^T, I_c^T]^T$ , where  $I_x$  is the one-hot representation to encode the value of  $x$ . Given that  $A, B, C, a, b$  and  $c$  are all smaller than 50 in the experiment, the dimension of  $n_t$  is 300. The initial query  $q$  is obtained by  $q = E[q]$ , where  $E$  is a query embedding lookup table and  $E[x]$  indicates the  $x$ -th column. The query embedding dimension is set to 64. In the three glass puzzle, there are 13 actions in total: fill one container to its capacity, empty one container, pour one container into another container, and a STOP action to terminate the game. We set the maximum length of an action sequence (i.e., the search horizon) to be 12, where only the STOP action can be taken on the final step. After the STOP action has been taken, the system evaluates the action sequence and assigns a reward  $r = 1$  if the final status is a success, otherwise  $r = 0$ . The  $f_{\theta_s}$  and  $f_{\theta_A}$  functions are modeled by two different DNNs with the same architecture: two fully-connected layers with 32 hidden dimensions and ReLU activation function.  $f_{\theta_v}$  is a two fully-connected layers with 16 hidden dimensions, where the first hidden layer is with ReLU activation function and the output layer is with linear activation function.  $f_{\theta_q}$  is modeled by a GRU with hidden size 64. The hyperparameters in PUCT are set to  $c = 0.5$  and  $\beta = 0.2$ . We use the ADAM optimization algorithm with learning rate 0.0005 during training, and we set the mini-batch size to 8.

Table 3: A List of Actions for Each Container in the Three Glass Puzzle. The agent can also determine to take the STOP action to terminate the game.

Empty A	Fill A	Pour A to B	Pour A to C
Empty B	Fill B	Pour B to A	Pour B to C
Empty C	Fill C	Pour C to A	Pour C to B

Table 4: Knowledge base completion datasets statistics.

Dataset	# Train	# Test	# Relation	# Entity	avg. degree	median degree
WN18RR	86,835	3,134	11	40,943	2.19	2
NELL-995	154,213	3,992	200	75,492	4.07	1



(a) Test Beam / Rollout = 128 (b) Test Beam / Rollout = 300

Figure 8: Test Accuracy on Three Glass Puzzle task. Higher is better. PG stands for policy gradient.

## B.2.2 Knowledge Base Completion

**Statistics of the two datasets** The NELL-995 knowledge dataset contains 75,492 unique entities and 200 relations. WN18RR contains 93,003 triples with 40,943 entities and 11 relations. The detailed statistics are shown in Table 4.

**Experiment settings and hyperparameters** For the proposed M-Walk, we set the entity embedding dimension to 4 and relation embedding dimension to 64. The maximum length of the graph walking path (i.e., the search horizon) is 8 in the NELL-995 dataset, and 5 in the WN18RR dataset. After the STOP action has been taken, the system evaluates the action sequence and assigns a reward  $r = 1$  if the agent reaches the target node, otherwise  $r = 0$ . The initial query  $q$  is the concatenation of the entity embedding vector and the relation embedding vector. The  $f_{\theta_S}$  and  $f_{\theta_A}$  functions are modeled by two different DNNs with the same architecture: two fully-connected layers with 64 hidden dimensions and the ReLU activation function.  $f_{\theta_v}$  is two fully-connected layers with 16 hidden dimensions, where the first hidden layer uses a Tanh activation function and the output layer uses a linear activation function.  $f_{\theta_q}$  is modeled by a GRU with hidden size 64. The hyperparameters in PUCT are set to  $c = 2$  and  $\beta = 0.5$ . We roll out 32 MCTS paths in both training and testing in the NELL-995 dataset and 128 MCTS paths in the WN18RR dataset. We use the ADAM optimization algorithm for model training with learning rate 0.0001, and we set the mini-batch size to 8.

## C Additional Experiments

### C.1 The Three Glass Puzzle task under different settings

We now conduct more experiments on the Three Glass Puzzle task under different settings. First, to see how fast M-Walk converges, we show in Figure 8 the learning curves of M-Walk and PG. It shows that M-Walk converges much faster than PG and achieves better results on this task. In Table 5, we report the test accuracy of M-Walk and vanilla policy gradient (REINFORCE/PG) with different beam search sizes and different MCTS rollouts during testing. The number of MCTS simulations for training M-Walk is fixed to be 32. We observe that M-Walk with MCTS achieves the best test accuracy overall. In addition, with larger beam search sizes and MCTS rollouts, the test accuracy improves substantially. Furthermore, replacing the MCTS in M-Walk by beam search at test time

Table 5: Three Glass Puzzle Test Accuracy (%), where “Beam” denotes beam search.

Size	1	10	50	100	200	300	400
PG (Beam)	9.3 (2.1)	30.7 (4.5)	39.3 (3.2)	45.3 (4.5)	47.7 (3.2)	48.7 (3.2)	49.0 (2.6)
M-Walk (Beam)	18.0 (1.7)	46.0 (7.0)	60.3 (7.8)	67.0 (7.0)	69.0 (6.2)	69.3 (6.4)	71.7 (4.5)
M-Walk (MCTS)	<b>18.0</b> (1.7)	<b>63.3</b> (5.0)	<b>84.3</b> (3.1)	<b>90.7</b> (2.5)	<b>95.0</b> (2.6)	<b>96.3</b> (1.5)	<b>99.0</b> (1.0)

Table 6: BFS, DFS and M-Walk on Three Glass Puzzle.

Method	Average # Steps	Max # Steps
BFS	264.7	1030
DFS	192.2	1453
M-Walk	94.9	897

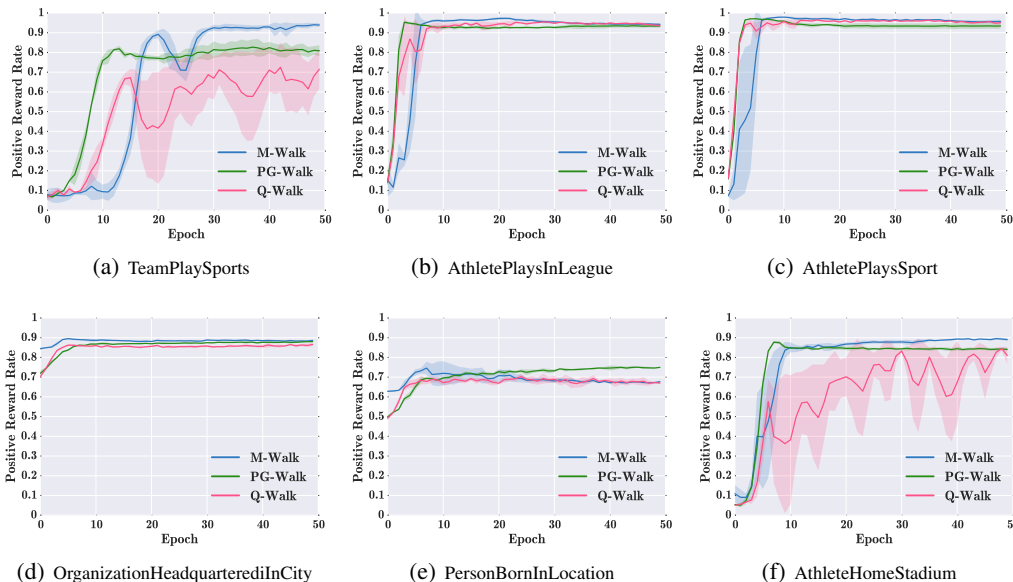


Figure 9: The positive reward rate during training (i.e., percentage of trajectories with positive reward during training) on the NELL-995 task.

degrades the performance greatly, which shows that MCTS is also very important for M-Walk at test time.

As we mentioned earlier, the conventional graph traversal algorithms such as Breadth-First Search (BFS) and Depth-First Search (DFS) cannot be applied to the graph walking problem, because the ground truth target node is not known at test time. However, to understand how quickly M-Walk with MCTS could find the correct target node, we compare it with BFS and DFS in the following cheating setup. Specifically, we apply BFS and DFS to the test set of the Three Glass Puzzle task by disclosing the target node to them. In Table 6, we report the average traversal steps and maximum steps to reach the target node. The M-Walk with MCTS algorithm is able to find the target node more efficiently than BFS and DFS.

### C.1.1 Knowledge Graph Link Prediction

In this section, we provide more experiment results for the two KBC tasks to support our analysis. In Figure 9, we show the positive reward rate during training on the NELL995 task. And in Figure 10, we provide more hyperparameter analysis (search horizon and MCTS simulation number) and training time analysis.

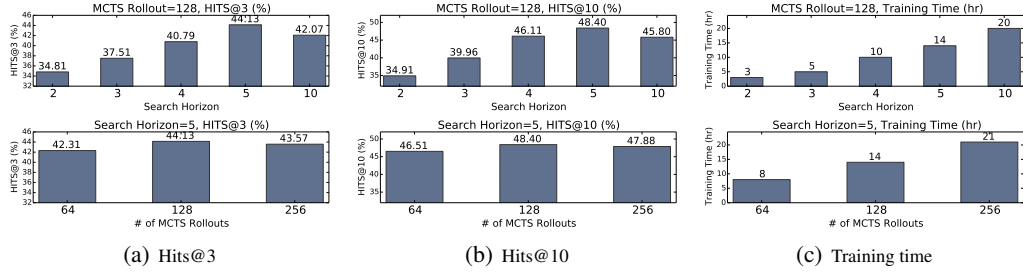


Figure 10: M-Walk hyperparameter and error analysis on WN18RR.

(i) **Search different paths after a dead end:** coach andrew brunette  $\xrightarrow{\text{athlethehomestadium}}$  ?

a) coach andrew brunette  $\xrightarrow{\text{athletheplaysforteam}}$  sportsteam blackhawks  $\xrightarrow{\text{atlocation}}$  county chicago  $\xrightarrow{\text{ATLOCATION}^{-1}}$  stadiumoreventvenue orchestra hall  $\xrightarrow{\text{atlocation}}$  county chicago  $\xrightarrow{\text{STADIUMLOCATEDINCITY}^{-1}}$  stadiumoreventvenue united center  $\xrightarrow{\text{TEAMHOMESTADIUM}^{-1}}$  sportsteam chicago bulls  $\xrightarrow{\text{TEAMHOMESTADIUM}^{-1}}$  stadiumoreventvenue united center, ( $V(s_T)=0.3832$ , False)

b) coach andrew brunette  $\xrightarrow{\text{athletheplaysforteam}}$  sportsteam blackhawks  $\xrightarrow{\text{athletheplaysforteam}^{-1}}$  athlete rich hill  $\xrightarrow{\text{ATHLETHEPLAYSFORTEAM}}$  sportsteam blackhawks  $\xrightarrow{\text{TEAMHOMESTADIUM}}$  stadiumoreventvenue wrigley field, ( $V(s_T)=0.9093$ , True)

---

ii) **Search over multiple paths to the target entity:** ceo evan williams  $\xrightarrow{\text{personleadsorganization}}$  ?

a) ceo evan williams  $\xrightarrow{\text{worksfor}}$  company twitter, ( $V(s_T)=0.9166$ , True)

b) ceo evan williams  $\xrightarrow{\text{worksfor}}$  company twitter  $\xrightarrow{\text{organizationterminatedperson}}$  ceo jack dorsey  $\xrightarrow{\text{cecof}}$  company twitter, ( $V(s_T)=0.8693$ , True)

---

iii) **worksfor**  $\leftrightarrow$  **organizationhireperson** $^{-1}$ : ceo garo h armen  $\xrightarrow{\text{worksfor}}$  ?

ceo garo h armen  $\xrightarrow{\text{organizationhireperson}^{-1}}$  biotechcompany antigenics inc, ( $V(s_T)=0.9351$ , True)

Table 7: Examples of paths found by M-Walk on the NELL-995 dataset. M-Walk can learn to traverse multiple paths to reach the target node (example i) and learn to explore new paths when reach a dead end (example ii).

## C.2 The Reasoning (Traversal) Paths

In Tables 8 and 9, we show several traversal paths made by the ReinforceWalk model in the test set of Three Glass Puzzle dataset. Furthermore, in Table 7, we show the reasoning paths of M-Walk on the NELL995 dataset.

Table 8: M-Walk Traversal Paths in Three Glass Puzzle, where “Index” stands for MCTS Path Index.

Query	Index	M-Walk Action Sequence	Estimated V
$(A, B, C, q)$ $= (14, 45, 47, 15)$	0	$(0, 0, 0) \rightarrow (14, 0, 0) \rightarrow (0, 14, 0) \rightarrow (14, 14, 0) \rightarrow (0, 14, 14) \rightarrow (14, 14, 14) \rightarrow (0, 14, 28) \rightarrow (14, 14, 14) \rightarrow (0, 14, 28) \rightarrow (14, 0, 28) \rightarrow (14, 45, 28) \rightarrow (14, 26, 47) \rightarrow \text{END}$	$1.13\text{e-}6$
	1	$(0, 0, 0) \rightarrow (0, 0, 47) \rightarrow (14, 0, 33) \rightarrow (0, 14, 33) \rightarrow (14, 14, 19) \rightarrow (0, 14, 19) \rightarrow (14, 0, 19) \rightarrow (14, 19, 0) \rightarrow (14, 19, 47) \rightarrow (14, 45, 21) \rightarrow (14, 0, 21) \rightarrow (0, 14, 21) \rightarrow \text{END}$	$6.31\text{e-}8$
	...	...	...
	14	$(0, 0, 0) \rightarrow (0, 45, 0) \rightarrow (0, 0, 45) \rightarrow (14, 0, 31) \rightarrow (14, 45, 31) \rightarrow (14, 29, 47) \rightarrow (14, 29, 0) \rightarrow (0, 29, 14) \rightarrow (14, 15, 14) \rightarrow \text{END}$	$0.9999$
	...	...	...

Table 9: M-Walk Traversal Paths in Three Glass Puzzle, where “Index” stands for MCTS Path Index.

Query	Index	M-Walk Action Sequence	Estimated V
$(A, B, C, q)$ $= (11, 15, 30, 8)$	0	$(0, 0, 0) \rightarrow (0, 0, 30) \rightarrow (11, 0, 30) \rightarrow (0, 11, 30) \rightarrow (11, 11, 19)$ $\rightarrow (0, 11, 30) \rightarrow (11, 11, 19) \rightarrow (0, 11, 30) \rightarrow (11, 0, 30)$ $\rightarrow (0, 11, 30) \rightarrow (11, 11, 30) \rightarrow (7, 15, 30) \rightarrow \text{END}$	2.13e-8
	1	$(0, 0, 0) \rightarrow (0, 0, 15) \rightarrow (0, 0, 15) \rightarrow (0, 15, 15) \rightarrow (11, 4, 15)$ $\rightarrow (0, 4, 26) \rightarrow (4, 0, 26) \rightarrow (4, 15, 26) \rightarrow (11, 8, 26) \rightarrow \text{END}$	0.999
	...	...	...
	4	$(0, 0, 0) \rightarrow (11, 0, 0) \rightarrow (0, 0, 11) \rightarrow (11, 0, 11) \rightarrow (0, 11, 11)$ $\rightarrow (11, 11, 11) \rightarrow (0, 11, 22) \rightarrow (11, 11, 11) \rightarrow (7, 15, 11) \rightarrow$ $(7, 0, 11) \rightarrow (7, 15, 11) \rightarrow (7, 15, 30) \rightarrow \text{END}$	1.72e-8
	...	...	...